JOURNAL OF MATERIALS SCIENCE 7 (1972) 822–835

Origin of contrast effects in the electron microscopy of polymers

Part 2: *Polyethylene spherulites*

D. T. GRUBB, A. KELLER, F.R.S.
University of Bristol, H. H. Wills Physics Laboratory, Tyndall Avenue, Bristol, UK

Self-supported thin spherulitic films of polyethylene change their form dramatically during observation in the transmission electron microscope. Crystalline diffraction contrast disappears, then details of the radiating fibrils become visible. The circumferential bands of a banded spherulite are originally visible in the diffraction contrast, and after this has faded they reappear with stronger contrast, but reversed. At the same time each spherulite in the originally flat specimen becomes conical in shape. The same topographical changes are observed in the scanning electron microscope.

All the effects can be explained by assuming that the crystalline sub-units of the spherulites deform in the electron beam in the same way as single crystals do. The anisotropic deformation of polyethylene single crystals in the electron microscope was described in Part 1 of this paper [1].

1. Introduction

Part 1 of this paper [1] described the deformation and contrast changes which occurred during observation of lamellar single crystals of polyethylene (PE) in the electron microscope. Deformation and contrast changes are observed in every type of PE sample in the electron microscope. It was stated in Part 1 that the simple behaviour of a single crystal could be used as a model to explain the effects seen in complex systems built of lamellar crystals. The second part of this paper describes a test of this statement, where the single crystal behaviour has been applied to explain spherulite behaviour. Spherulites are suitable model structures for lamellar aggregates, since their own internal structure is reasonably well understood and at the same time they are themselves important structural units.

Spherulites are the characteristic structural elements arising from crystallization of polymers from the melt, and it was in spherulitic specimens that the problem of radiation-induced contrast changes was first described [2]. Spherulites are normally distinguished by the "maltese cross" appearance when observed between crossed polars in the optical microscope. The dark areas of the cross remain parallel and perpendicular to the plane of polarization so the birefringent units are arranged symmetrically. In the dark areas the index ellipsoid axes are parallel to the polarizer and analyser directions. If the long axis of the ellipsoid is radial, the spherulite is called positive; if tangential, negative. PE spherulites are negative indicating that the molecular chains are tangential.

A system of concentric dark rings or bands is often seen, superimposed on the dark cross [3-6] and these arise in the following manner. The birefringent units periodically vary in orientation, twisting about the radial growth direction. The period and phase is the same along every radius, so there are circumferential bands where the orientation is the same. When the index ellipsoids are positioned so that the section perpendicular to the incident light is circular, or nearly so, the band will be dark between crossed polars. In the case of PE, almost uniaxial and with negative spherulites, the dark bands will correspond to localities where the molecular chains are parallel to the incident light. Electron micrographs of spherulitic films showing twisted lamellae have been taken as support for this model [4, 7] without consideration of why the

structure should be visible when electrons and not polarized light are used to form the image.

At one stage an alternative model of the structure of banded spherulites was proposed, which involved a cyclic variation of the amorphous content along a radius. The dark bands that appear in the polarizing microscope would then correspond to localities where the material is largely amorphous. Claver *et al* [8] noted the visibility of the bands in the electron microscope, and remarked that this could not be associated with variations in birefringence. This argument for the alternative model was weakened by the fact that thin cast films such as they used have a periodic variation in thickness corresponding to the band periodicity. The thicker regions are bright when observed between crossed polars [9]. The model was revived when bands were seen in ultramicrotomed section of PE, cut to a uniform thickness [10].

Dlugosz and Keller [2] recognized that beam damage effects had overwhelming importance in the electron microscopy of spherulites. They observed that ultramicrotomed sections of PE had little or no contrast initially; the bands and lamellar detail appeared on irradiation. They also showed that an initially smooth cut surface developed undulations corresponding to the band structure on irradiation in the scanning electron microscope.

To follow the process of radiation damage in detail, it is necessary to have very thin specimens. In the present work these were prepared in the simplest possible way, by allowing a thin film of molten PE to cool. Crystallization proceeds in a similar manner to that in the bulk, but is constrained to occur in a plane. Thus each two-dimensional "spherulite" grows outwards with a circular boundary, instead of a spherical one. Each "spherulite" is like the diametral section of a true spherulite, but with the small modification that nucleation will occur at the surface of the film rather than the centre, so that radial growth is inclined to the plane of the film [6, 11]. Also, as mentioned above, the thickness of the film is not constant. All this must be kept in mind when these crystalline assemblies are, for convenience, referred to as spherulites.

2. Experimental

2.1. Specimen preparation

To prepare a sufficiently thin continuous film the polymer, Marle × 6009, was first dissolved in xylene at a concentration of about 0.01 g/ml and cooled to form a slurry. PE sticks to any solid substrate it is cast on, so a liquid surface was used. Ortho-phosphoric acid and glycerol are suitable; a few drops of the liquid were put on a microscope slide which was on a "Kofler" hot-bench. A drop of the slurry was allowed to fall on the hot liquid surface and while the solvent evaporated, the drop spread and the polymer melted. The PE film produced in this way was solidified by moving the slide down towards the cold end of the hot-bench. The solid film was floated off on a water surface and allowed to stand while the support liquid dispersed. The film was then picked up on a clean slide, and thin areas selected in the optical microscope. Regions which are thin enough for transmission electron microscopy are almost invisible in the optical microscope. These areas were cut out, floated off on water again, and picked up on a 50-mesh grid. For scanning electron microscope specimens, the same procedure was used, and the grid was stuck to a specimen stub.

The films were not metal-coated or shadowed for the transmission electron microscope, as this could give rise to artefacts. There was therefore some charging, especially in thicker regions, but this did not affect the quality of the image. For the scanning electron microscope, specimens were coated with gold as they rotated. Only a small amount was deposited at one time, and the minimum thickness which prevented charging was found by trial and error.

2.2. Electron microscopy

As in Part 1 of this paper, the transmission electron microscope used was a Philips EM200. For this part of the work the goniometer facility for rapid tilting of the specimens $\pm$ 50° was particularly important. The beam current was measured with the exposure-meter of the microscope [12] and together with the magnification this gives the radiation dose at the specimen.

Radiation damage effects in the scanning electron microscope occurred quite slowly, taking typically 10 min at 1000 times magnification and 15 kV. However, to get a picture of undamaged material at 5000 × or over it was necessary to focus on one area and to photograph another without refocusing. This is standard practice in transmission electron microscopy of polymers [13]. Focusing at the highest possible magnification, then reducing the magnification and immediately taking a picture, gives a micrograph showing a damaged central square with an

Figure 1 Stereo pair of a spherulite of polyethylene after radiation damage in the electron microscope, 6° tilt between the pair.

undamaged border. This technique was used in a study of radiation damage of polyoxymethylene in the scanning electron microscope [14], and in that material some structural features were exposed by beam damage.

3. Observations in the electron microscopes

Fig. 1 is a stereo pair of a spherulite taken with an angular separation of 6° after a very long exposure to the beam. The standard angular separation for stereo pairs (eye separation)/(distance of closest vision), is about 12°. Thus the stereo depth in Fig. 1 should be about half that of the real object. Since a stereo viewer may not be to hand Fig. 2 shows the same spherulite, tilted through 60°. The spherulite was near the edge of the specimen so it is clearly seen to be conical, with a semi-angle of 47°. The conical shape is not perfectly regular, and has a distorted tip. Some smaller bumps in the specimen are centred on points where three spherulites meet. The circumferential bands are clearly visible, and the dark bands appear to consist of small radial units. This spherulite is larger and more regular than most, but the behaviour is completely typical.

All the specimens, including non-banded spherulites, are initially flat and become covered with conical hills and craters as radiation proceeds. Sometimes the specimen curls up so that, on tilting, a part of it becomes vertical. The profile of this part then becomes visible. Fig. 3 was taken under these conditions and shows the rough surface of an irradiated specimen. All the conical hills have the same semi-angle, 45° ± 3°. The specimen changes too rapidly to get a stereo pair of it in its original state, but the scanning electron microscope gives micrographs of immediate three-dimensional appearance. Fig. 4 is such a picture, taken at low magnification after a central area has been heavily irradiated at higher magnification. The scanning electron beam produces a uniformly irradiated area with sharp cut-off at well-defined boundaries. The border, lightly irradiated by only a few scans at low magnification, is generally flat; the spherulites are clearly outlined by grooves at the boundaries between them, and there are slight bumps or hollows at the centres of some spherulites. It is clear that the conical bumps which stand out from the specimen plane are a product of the irradiation. Fig. 5 is a more detailed view of a heavily irradiated area in the scanning microscope.

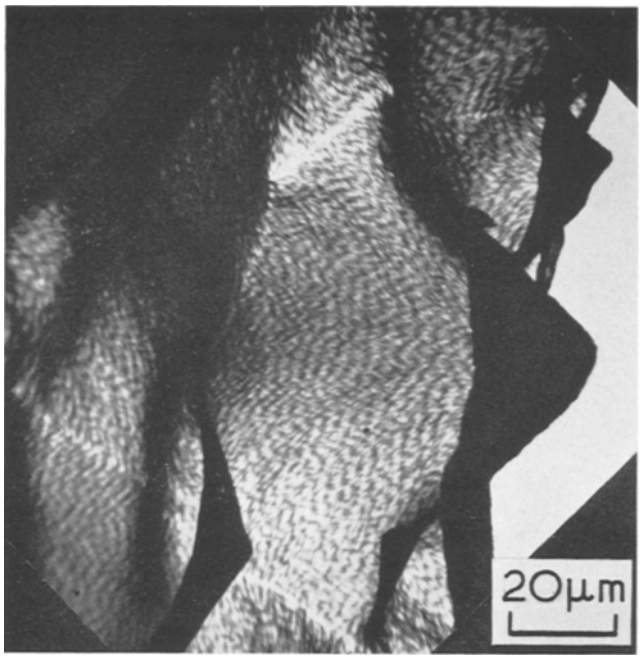

Figure 2 The same area as in Fig. 1, but tilted by 60°, to show the conical shape.

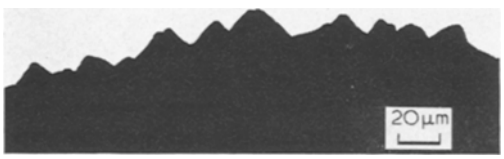

Figure 3 Low magnification electron micrograph of the surface profile of an irradiated spherulitic film.

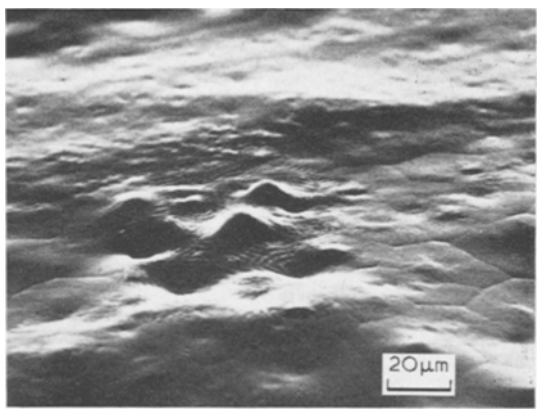

Figure 4 Scanning electron micrograph of a spherulitic film of polyethylene, with a central square previously observed (and thus irradiated) at higher magnification.

The specimen was tilted to 60° in this picture, so that it is equivalent to the transmission micrograph in Fig. 2. The coating of gold and the lower accelerating voltage make the specimen opaque in Fig. 5, and makes the surface features show up. The shaggy appearance of radiating fibrils stands out very well, and the bands now show as undulations in the surface, confirming that their contrast in the transmission microscope is due to thickness variations in the specimen. The semi-angle of the cones is the same as before, about 42°, but there is an important difference. The conical shape extends only half way out from the centre of the spherulite; it rises sharply from an outer ring which is almost flat. This behaviour is not confined to the scanning microscope, it is common in the transmission microscope as well, and occurs when the irradiated area is small and in the middle of the specimen (as in Fig. 4). The contrary behaviour, with spherulites going completely conical, as in Figs. 1, 2 and 3, occurs when a large area near the edge of a specimen is irradiated, and is associated with an overall contraction of the irradiated area.

Figs. 6b and c are a stereo pair of 6° separation showing the behaviour of a small irradiated area in the transmission microscope. There is a flat outer region in each spherulite, and an inner cone

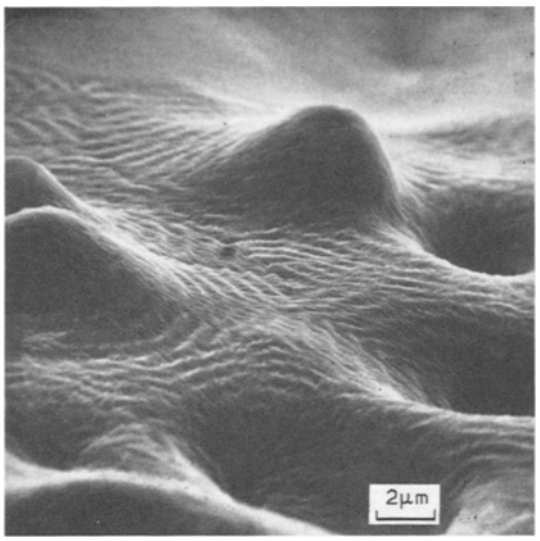

Figure 5 Scanning electron micrograph of a spherulitic film of polyethylene, showing structures induced by the beam in more detail.

of semi-angle 49° ± 9°. The general features can be followed without a stereo viewer by noticing the denser ring round the centre of each spherulite. This is where the specimen is oblique, and the projected thickness is greater. Fig. 6a is of the same area, taken first at very low radiation doses when diffraction contrast is still visible. The pattern of spherulite boundaries has hardly changed between Figs. 6a and b. A straight boundary section in Fig. 6a is on average 5 ± 3% shorter in Fig. 6b. In the flat outer ring of each spherulite there has been a radial expansion of about 20%. These figures varied from region to region of the specimen, and the irregularity of most spherulites, as in Fig. 6, makes accurate determination of the radial expansion difficult. Some specimens were exposed to tungsten oxide smoke rising from a burning tungsten filament, and this produces many small stable particles on the surface. Using these as markers, and measuring only the few regular spherulites, the mean radial expansion in the flat region was 12 ± 5%, and the conical region extended out to 0.4 ± 0.1 of the total radius.

The bands are visible in Fig. 6a but there is little sign of a radiating fibrillar structure. The contrast of the bands reverses between Figs. 6a and b, but this is not immediately clear. Fig. 7 shows a detail of a banded spherulite before and after irradiation in the transmission electron microscope. This specimen had been treated with tungsten oxide smoke and these markers make the reversal of contrast between Figs. 7a and b quite clear.

Irradiation in the transmission microscope brings out details of radiating lamellae particularly well in non-banded spherulites. Figs. 8a to d are sequential photographs of such a specimen taken at increasing radiation dose. The specimen was unusually stable in Fig. 8a, so the initial diffraction contrast is seen to be a jumble of dark fine lines. A dark spot indicates that a crystallite is diffracting strongly, so the lines will be loci of points where the twisting lamellae are correctly oriented for diffraction. Figs. 8b and c show the intermediate stages of low contrast and specimen motion which had been omitted from Figs. 6 and 7. In Fig. 8d the lamellae are very clear, seem to be twisting, and appear most distinctly when they are narrow, that is, edge-on. Comparison of Figs. 8a and d shows that the dark lines of diffraction contrast are most common in areas light and featureless in Fig. 8d. This behaviour is the same as the contrast reversal of a banded spherulite shown in Fig. 7.

The lamellar structure always shows up with high contrast in irradiated areas in the scanning microscope. In Fig. 9a, a high magnification picture of the centre of Fig. 5, the specimen is tilted to 60° so that the view is along a tangent of one spherulite, and nearly along a tangent of the adjacent one. Fig. 9b is an area nearby, at the same magnification and tilt, but here the view is along a radius. From Fig. 9a, the height from the peaks to the valleys is 0.2 μm, and the profile is smooth, regular, and sinusoidal. The twist of the lamellae in Fig. 9b is right-handed since the centre of the spherulite is below the edge of the picture. The bright lines appear to be about 500Å wide, but this is the instrumental resolution under the conditions of taking Fig. 9, and therefore an upper limit on the real width. The brightness of these lines indicates, in the scanning electron microscope, a feature standing proud of the surface. Adjacent bright lines are sometimes not resolved, and may be 0.6 μm apart, but the average is about 0.2 μm. The tangential extent of an isolated bright line, as at the lower right of Fig. 9b, gives a lower limit for the width of a lamella, usually about 0.5 μm.

Fig. 10 is an optical micrograph, taken in transmission with crossed polars of a specimen after observation in the scanning electron microscope. It shows an area such as that in Fig. 4. The birefringence has largely disappeared from the

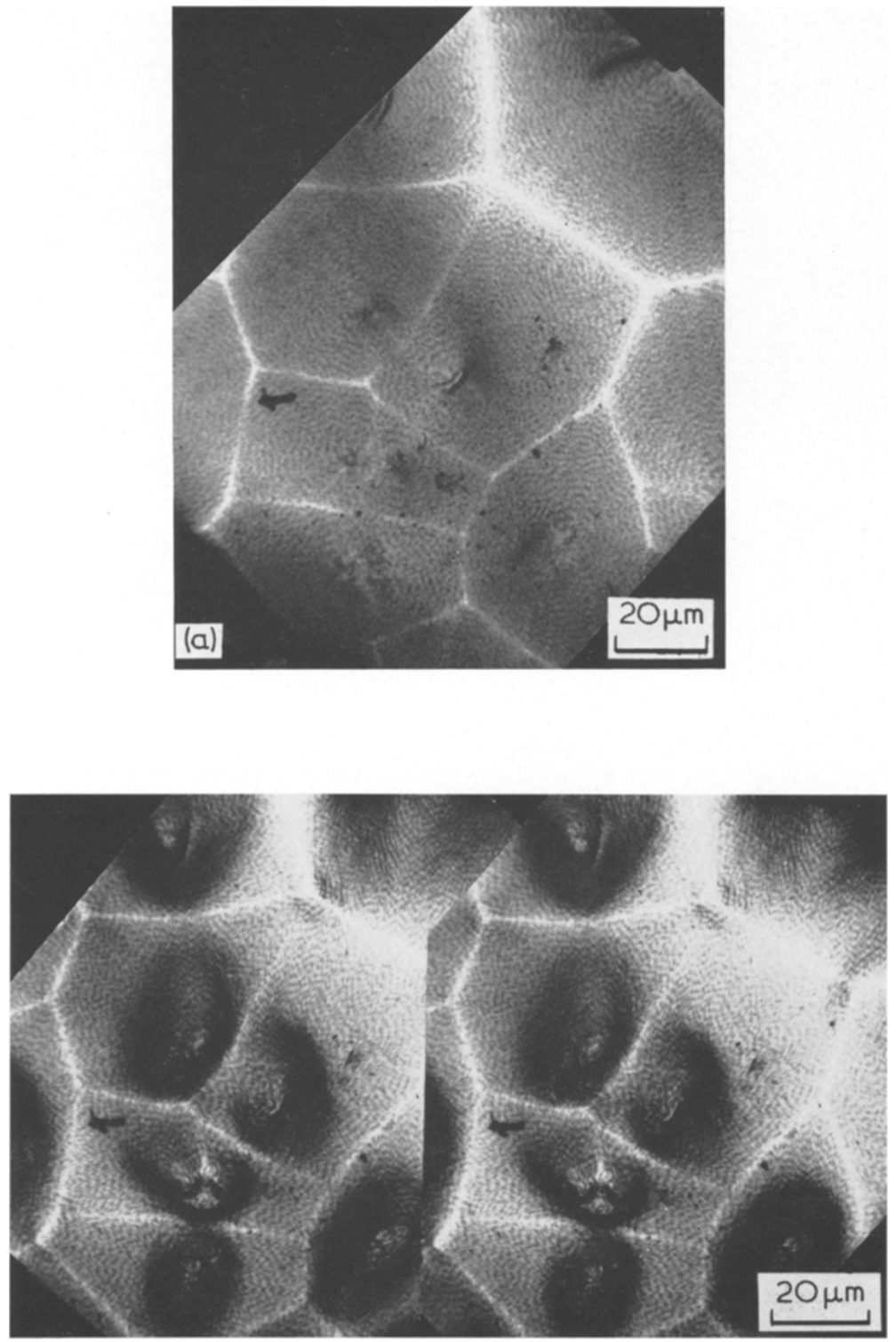

Figure 6 Transmission electron micrographs of a spherulitic film of polyethylene, firmly constrained. (a) Before significant radiation damage. (b) Stereo pair of 6° separation after radiation damage.

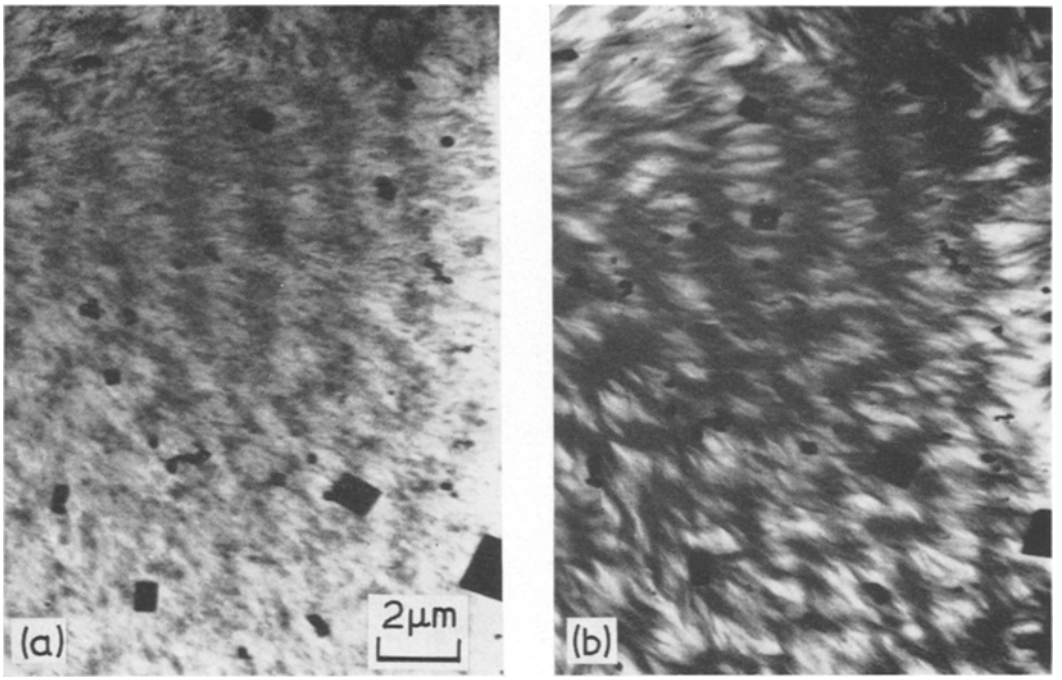

Figure 7 Detail of polyethylene spherulite in the transmission electron microscope, to show contrast reversal between (a) Original appearance, radiation dose $< 30\ Cm^{-2}$ at 100 kV. (b) Final appearance, radiation dose $> 300\ Cm^{-2}$ at 100 kV.

square which has been irradiated, and this means that the crystallinity has been destroyed. The remaining traces of birefringence may mean that the 20 kV electrons have not penetrated to the bottom of the specimen, so there is still a thin undamaged layer there.

4. Predicted behaviour in the electron microscopes

4.1. Model for prediction

According to the presently accepted model, spherulites consist of radiating lamellar units, with the *b* direction radial. The *a* and *c* directions are distributed about the tangential plane. When a two-dimensional "spherulite" or a spherulite section is seen to be banded in the polarizing optical microscope there is a further degree of ordering. Namely, the lamellae vary their orientation periodically with respect to the viewing direction along any given radius. In dark bands the birefringence is low because the molecular chain direction *c* is perpendicular to the specimen plane, and *a* lies in it. In the bright bands *c* lies in the plane, and *a* is perpendicular to it. The lamellae twist continuously and regularly from one orientation to the other.

The lamellae are very similar to solution-grown lamellar crystals, being thin sheets with the lamellar normal nearly parallel to *c*. Keller and Sawada [15] found that the *c*-axis was inclined with respect to the lamellar normal by rotation about *b* through 15 to 20° in rapidly cooled specimens. All the specimens described here were rapidly cooled, so this degree of obliquity should be present. Such a small obliquity would make a negligible difference to the arguments which follow. Consequently a good description of the structure is that in dark bands the lamellae lie nearly parallel to the specimen plane, and can be described as "flat-on". In bright bands they lie nearly perpendicular to the specimen plane, or "edge-on". The effect of greater chain obliquity is discussed in Section 4.6.

To this structural model of a spherulite we apply the irradiation behaviour of a solution-grown lamellar crystal, by assuming that the lamellae in spherulites behave in exactly the same way. It was shown in the first part of this paper [1] that a solution-grown lamella of PE, when lightly constrained and exposed to the intense radiation flux of an electron microscope,

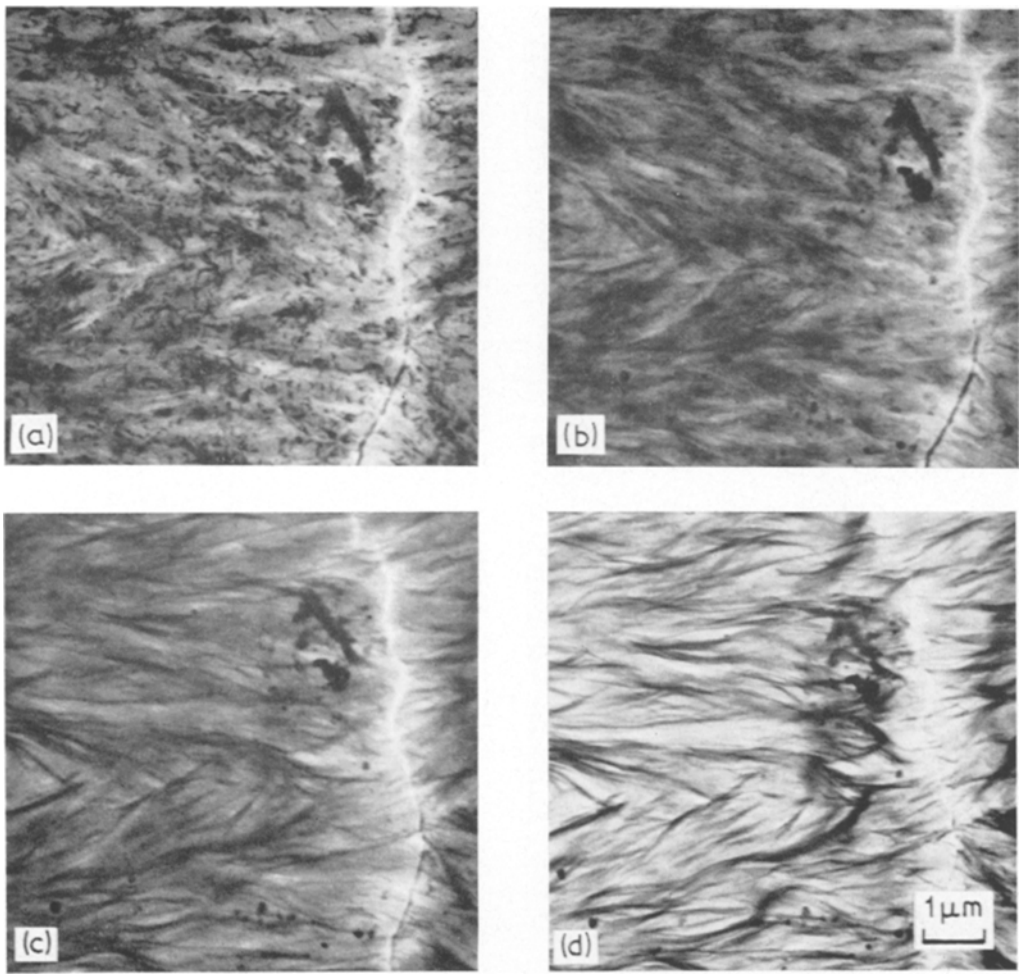

Figure 8 Radiation damage sequence of a detail from an unbanded spherulite, taken at 80 kV. (a) 1 to 6 Cm^{-2}. (b) 28 to 34 Cm^{-2}. (c) 69 to 75 Cm^{-2}. (d) 240 to 256 Cm^{-2}.

expanded uniformly in its own plane by up to 23%. Indications were that the volume of the material was reduced slightly, by 5%, at the same time, so that a contraction of nearly 40% along the molecular chain direction, *c*, was implied.

4.2. Unconstrained spherulite

Consider an isolated thin disc-shaped spherulite with no banding, and assume that the radiating crystalline lamellae behave as above. The radii, along *b*, will expand by 23%, and there will be a contraction in the tangential plane. In spherulites with no banding, orientation in this plane is randomized, so if the specimen volume is reduced by 5%, the linear contraction in the plane is $1 - (0.95/1.23)^{\frac{1}{2}}$, or 12%. This means that the disc becomes thinner by 12% and a circumferential path traversing the material is reduced by the same amount. This can occur in two ways. 1. Voids form, and unless the spherulite is going to split up, they will be evenly dispersed between lamellae or lamellar packets. 2. The material remains continuous, and the circumference itself is reduced. Circumference equals $2\pi \times$ radius, so the radius of the disc should fall by 12%, but at the same time the distance from the centre to any point at the edge increases by 23%. This can only happen if the disc becomes non-planar, and by its symmetry it must become a cone. The semi-angle of the cone is given by $\sin^{-1}(0.88/1.23) = 46°$. This is in excellent agreement with the experi-

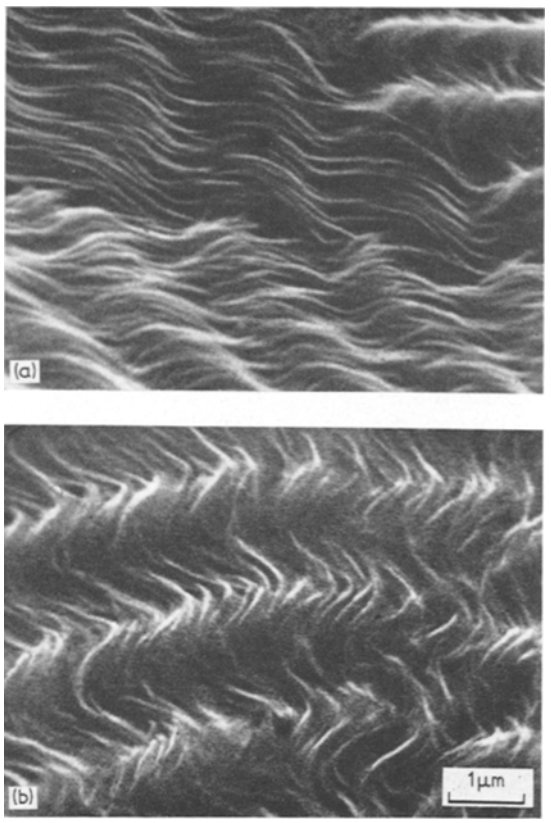

Figure 9 Scanning electron micrographs of lamellar detail visible in irradiated areas. (a) Enlargement of central region of Fig. 5. (b) Adjacent region, looking along spherulite radius.

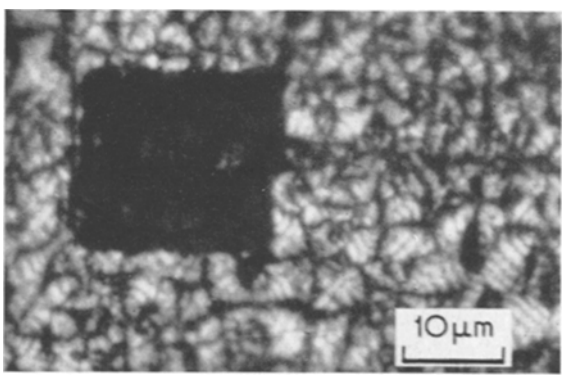

Figure 10 Optical micrograph of a spherulitic film after observation in the scanning electron microscope. Birefringence is removed in the irradiated area.

mental value of 45° ± 3° found for banded and non-banded spherulites. The fine-scale ordering of lamellar twisting into bands does not apparently affect this large-scale behaviour.

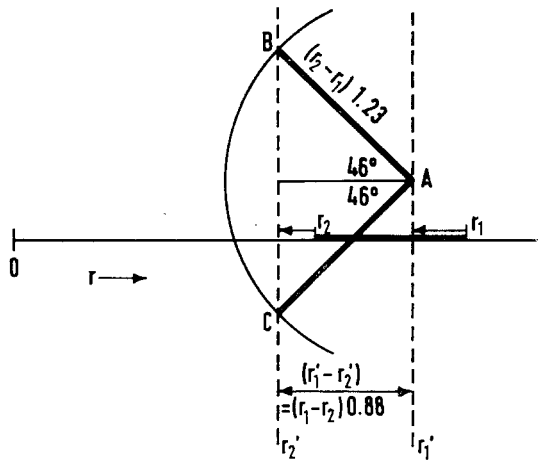

Figure 11 Schematic cross-section through an unconstrained spherulite.

Fig. 11 is a diagram of a cross-section of an unconstrained spherulite. The centre, $r = 0$, is at the left, and the behaviour of a section between r_1 and r_2 is shown. On irradiation, the circumferential contraction changes r_1 to r_1' and r_2 to r_2' where $r_1'/r_1 = r_2'/r_2 = 0.88$. However, the radial distances are measured from the perpendicular axis through $r = 0$, so unless it is assumed that some parts of the spherulite remain in the original plane, the section can lie anywhere between the dashed lines drawn though r_1' and r_2'. The radial expansion causes the section length to increase to $(r_1 - r_2)$ 1.23. Taking one end arbitrarily at point A, the arc $(r_1 - r_2)$ 1.23 intercepts the r_2' line at B and C, at + 46° and − 46°. Thus the whole spherulite becomes a cone, and can equally well point "up" or "down". Any section must remain straight, or bend discontinuously from + to − 46°, since the parts of a continuous bend would not be obeying these rules. Experimentally, all spherulites observed become conical, pointing either "up" or "down", and do not change direction at any intermediate radius.

The boundary of the spherulite will only remain planar if the spherulite is round. In reality the boundaries are polygonized by impingement on other spherulites, so each initially straight segment should end up as a parabola. A point where three spherulites meet should therefore stand out of the plane as a three-sided cusp (like Mont Blanc) as long as the three spherulites have

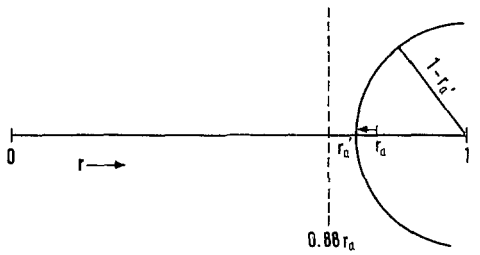

Figure 12 Schematic cross section through a spherulite with a fixed boundary.

all deformed to the same side of the specimen plane. In Figs. 1 and 2 such a cusp is visible, pointing "down" while the adjacent spherulites are cones pointing "up".

As nucleation occurs at the surface of the specimen, there must be a region at the very centre of the spherulite where the growth direction is inclined steeply to the specimen plane. This different orientation would cause a local radial contraction, and a flattened top to the cones. This is not observed; the tip of the cone usually has a pinched and irregular appearance. For example, in Fig. 6, only one of the spherulites has a rounded top. The prediction is not fulfilled because the model assumes that the spherulite is perfectly symmetrical right to the centre. In fact spherulites begin to grow in the form of a sheaf. The asymmetric region extends sufficiently for it to mask the effect of the thickness of the film.

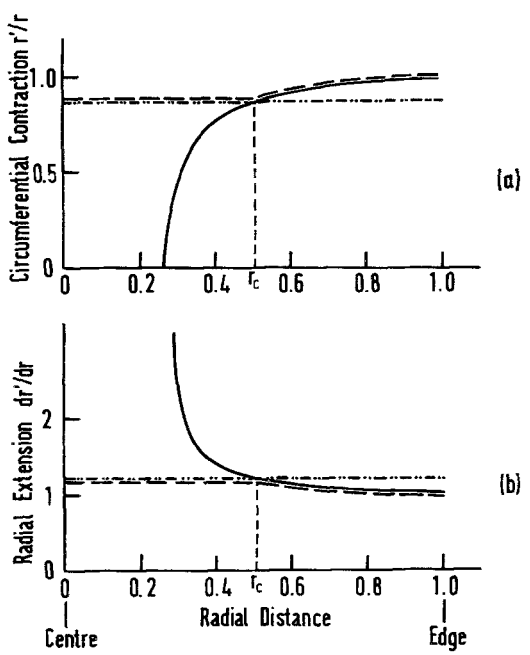

Figure 13 Calculated deformation of spherulites on irradiation.
– · – · · : unconstrained spherulite
——— : constrained spherulite, assuming that it remains flat after irradiation.
— — — : the actual constrained spherulite.

The model predicts an overall contraction of the specimen, 12% linear, or 25% in area. In lightly constrained areas, as in Figs. 1 and 2, considerable contraction is observed, as much as 22% linear contraction locally. The remaining constraints make the contraction very irregular and the specimen does not remain in one plane, so it has not been possible to measure the change in area for comparison with the predicted value.

4.3. Constrained spherulites

Consider a disc-shaped spherulite with no banding, as before, but now let the edge be held rigidly in position. This is a simple model of the case where the spherulite is surrounded by material which is not irradiated. There can be no circumferential contraction at the edge since it is held in a fixed position. The contraction perpendicular to the specimen plane is not affected by the constraint. As the volume change is constant, the radial expansion of material at the edge will be reduced to the amount allowed by the contraction perpendicular to the specimen plane. Thus material near the fixed edge becomes thinner and expands inwards. Fig. 12 shows a cross-section through a constrained spherulite, for comparison with Fig. 11. The centre, $r = 0$, is at the left and the fixed edge, $r = 1$, at the right. A small section at the edge, of length $(1 - r_a)$, will extend to $(1 - r_a')$, but whatever angle the section takes up this is not enough to permit the free circumferential contraction of material at r_a to $0.88\,r_a$. The nearest approach to this which reduces the effect of the constraint to the minimum is when the material remains in the original specimen plane. Then at r_a there is some circumferential contraction to r_a' and the local radial expansion will be greater than it is at the edge. The way in which the local radial expansion varies can be calculated as long as it is assumed that the specimen stays flat.

Consider a block of material originally at radial distance r, with thickness t and volume V. After irradiation these become r', t' and V'. If the specimen remains planar, the fractional circumferential contraction is given simply by $2\pi r'/2\pi r = r'/r$. The contraction in the tangential plane is therefore $r'/r \,.\, t'/t$. The local radial expansion is dr'/dr

$$\therefore \quad dr'/dr \,.\, r'/r \,.\, t'/t = V'/V$$

$$\therefore \quad dr'/dr = B \,.\, r/r'$$

where $B = V'/V \,.\, t/t'$, a constant.

Here the boundary condition of the fixed edge is $r' = 1$ at $r = 1$ so the solution in terms of the final radial position r' is

$$r'^2 = Br^2 - B + 1 \qquad (1)$$

Experimental values described above for the change in V and t are $V'/V = 0.95$, $t'/t = 0.88$. $\therefore B = 1.08$. The radial expansion and circumferential contraction predicted by Equation 1 using $B = 1.08$ are plotted on Fig. 13. The straight dotted lines on Fig. 13 are the constant values obtained in unconstrained spherulites. In both graphs in Fig. 13 the two lines intersect at a critical value of r, $r_c = 0.51$, for which $r_c' = 0.45$.

Thus in the region $1 > r > r_c$, the specimen behaves as described in Fig. 12. That is, circumferential contraction is limited to that allowed by the radial expansion inwards from the fixed edge. To reduce the effect of the constraint and maximize the contraction, the specimen will remain flat. Therefore Equation 1 describes the behaviour of a constrained spherulite for $1 > r > r_c$.

At $r = r_c$, the circumferential contraction of a free spherulite is just attainable if the specimen remains flat. At this position the dashed line in Fig. 12 is a tangent to the arc. As the free value of contraction is reached, the radial expansion is no longer restricted so the deformation in all directions is exactly that of the free spherulite (Fig. 13). Therefore no external constraints can act on material of $r < r_c$ and the inner region will behave like an unconstrained spherulite. As can be seen in Fig. 13, the deformations predicted by Equation 1 for $r < r_c$ are greater than those of a free spherulite. This is obviously wrong, but so is the assumption that the spherulite remains flat in this inner region. It has just been shown that the inner region behaves like an unconstrained spherulite, which according to the previous section, becomes conical.

The deformation should therefore follow the heavy dashed curves in Fig. 13, with a discontinuity of behaviour at $r = r_c$. After irradiation the discontinuity will be visible since within the new value of the critical radius, r_c', the spherulite should become a right circular cone of semi-angle 45° as before, while outside this critical radius the spherulite should remain flat and expand radially inwards from the fixed boundary.

This is observed qualitatively in constrained specimens such as Figs. 4 to 6, and there is also quantitative agreement with the predictions of this model. From Equation 1, if $r_c = 0.51$, $r_c' = 0.45$. r_c' has been measured experimentally using stereo pairs of transmission electron micrographs which gave $r_c' = 0.40 \pm 0.1$. The predicted value of the average radial extension in the flat region is

$$\frac{r_c - r_c'}{1 - r_c} \times 100 = 12.7\% \,.$$

The experimental value for this parameter is $12 \pm 5\%$.

When observing the irradiation of spherulitic specimens in the electron microscope, there is always a general impression of motion of material inwards, towards the centre of each spherulite. If the constraints are slight there is an overall contraction of each spherulite, leading to inwards motion. This treatment shows that even when the specimen is constrained so that there is no overall contraction, material still moves inwards.

4.4. Banded spherulites

As mentioned above, the banded structure does not affect the large scale changes. The bands themselves become visible, since where the lamellae are "edge-on" the specimen thickness is along a, which without constraints would expand by 23%. In the "flat-on" bands the specimen thickness is along c, which contracts by nearly 40% when free to do so. This would give a final thickness ratio of 2 to 1. In itself this accounts for the most salient observations, namely the visibility of the concentric banding and the development of this visibility by the electron beam.

The bands which are bright in the optical microscope are "edge-on", so they will finally appear dark in the electron microscope. The most intense diffraction spots from PE crystals are (1 1 0) and (2 0 0). These are most likely to be excited when the lamellae are "flat-on", with c parallel to the electron beam. Thus the darkest areas in the original bright field diffraction contrast will be "flat-on" regions, which end up thinner than the "edge-on" regions. The contrast will therefore reverse, as shown in Figs. 6 and 7.

This description is sufficient to explain the final contrast in general terms, but it is obvious that the lamellae in a spherulite are not free of constraints, and this will affect their behaviour. In Part 1 of this paper (Fig. 4 ref. 1) it was noted that a group of crystals, free to contract along c as usual, but prevented from expanding

in one direction in their own plane, expanded by 30%, much more than usual, in the other direction. The contraction along c was impeded by the constraint at right angles to it, because the usual increase in area is about 50%. To find the effects of mutual constraints, take as a very simple model of a segment of spherulite, a block $2 \times 1 \times 1$ in length, thickness and breadth, initially composed of two $1 \times 1 \times 1$ blocks, one exactly "flat-on" the other exactly "edge-on". In the unconstrained spherulite, there is a circumferential contraction of 12%, and a radial expansion of 23%, so the block initially $2 \times 1 \times 1$ will be finally $2.46 \times t \times 0.88$. If the volume drops by 5%, t, the mean thickness, is $2 \times 0.95/(0.88 \times 2.46)$, $= 0.88$. In the "edge-on" block, it is the c contraction which has been limited to 12%. If there were no other constraints the thickness and the length would increase equally, such that $x^2 \times 0.88 = 0.95$ $x = 1.04$ so the "edge-on" block would be $1.04 \times 1.04 \times 0.88$. In the "flat-on" block the c contraction is in the thickness direction and not directly impeded, but the a expansion is forced to be a 12% contraction. If this were the only constraint, the final length of this block would be given by $l \times 0.62 \times 0.88 = 0.95$, $l = 1.74$. But the total length of the two blocks would then be $1.04 + 1.74 = 2.78$, whereas it is fixed at 2.46. If the lengths of both blocks are reduced in proportion, they will be 0.92 and 1.54. Recalculating the thickness using these figures gives

	l	t	b	V
edge-on	0.92	× 1.17 ×	0.88	= 0.95
flat-on	1.54	× 0.70 ×	0.88	= 0.95

so that the final thickness ratio has been reduced from 2:1 to 5:3.

There is no reason for assuming that the mutual constraints interact in this particular way, and a realistic model would have to take into account the continuous twist of the lamellae, and all the intermediate oblique orientations. All that this calculation can show is that the internal constraints are not sufficient to invalidate the initial simple description of why the concentric banding becomes visible in the electron beam.

4.5. Lamellar visibility

In the previous sections, the spherulite has been treated as a homogeneous unit, but this is not so. It is composed of radiating crystalline lamellae with discontinuities between them. These discontinuities will be most important in the direction of the lamellar thickness. Not only is the thickness the smallest dimension, but during irradiation it is trying to contract.

Local constraints on "flat-on" lamellae restrict the expansion in the specimen plane, but not the reduction of specimen thickness. There is thus no tension on the lamellar interfaces, and they will stay together. Of course, with the lamellae perpendicular to the electron beam, they would not appear distinct even if they were separated. The "edge-on" case is quite different. Local constraints limit the overall contraction in the thickness direction, so that the interfaces are in tension. If they extend or give way under this tension, then the adjacent lamellae are freed from their constraint, and will contract more. Surrounding material will still limit the radial expansion, so there must be an associated additional expansion out of the specimen plane. "Edge-on" lamellae will therefore appear distinct, and much thicker than the adjacent material.

This effect is always observed in the transmission electron microscope, Figs. 7 and 8 for example. In the scanning electron microscope, Figs. 5 and 9, it is particularly clear that in banded spherulites there are undulations corresponding to the bands, and some radial units standing out from this surface.

4.6. Chain inclination

The basic explanation given in Part 1 of this paper [1] for the deformation of polymer lamellae induced by radiation was that the parallel extended chains within a crystal become disordered by radiation, so their length along the original chain direction is reduced. Therefore a crystal will contract along c and expand along a and b. If the chain direction, c, is rotated about b so that it is not nearly perpendicular to the plane of the lamella, the deformations measured along the unit cell axes will not be affected, but deformations measured in the plane, and perpendicular to the plane, of the lamella will be reduced. As stated in Section 4.1, the chain inclination in samples used for the present work is expected to be too small for this reduction to be significant [15]. However, under different crystallization conditions the chain inclination may be greater, so that its effect can no longer be neglected.

When the chain inclination is large, the properties described in Sections 4.2 and 4.3 will not be affected at all. The conical shape depends only on the properties of the lamellae averaged over all orientations about b. The bands will become visible exactly as described in Section 4.4, but the regions which become thickest must be described as "c-axis in specimen plane" and not "edge-on". Similarly the regions which initially diffract most and finally become thin are "c-axis perpendicular to specimen plane" and not "flat-on".

An observable change might be expected in the lamellar visibility described in Section 4.5, since

individual lamellae should be most visible when they are "edge-on" even when this is not the position for greatest expansion out of the specimen plane. Thus the region of greatest lamellar visibility should be displaced radially from the thickest band, where c lies in the specimen plane. However, the oblique contraction and expansion causes the lamellar plane to rotate towards the chain direction. If the original obliquity of the chain axis was 35° (the highest value observed by Keller and Sawada [15]) after irradiation, the lamellar normal will be only 15° from the original chain axis. The displacement between best lamellar visibility and the thickest band is reduced to less than half the original obliquity.

Experimentally, clearly visible lamellae are not confined to one particular region of the banding in either scanning or transmission electron microscopy. They are most common near the thickest bands, but are spread over a wide range. This means that there is considerable disorder within banded spherulites, enough to mask any effects of chain inclination. The local crystalline diffraction contrast from sections of bulk PE microtomed at low temperature also indicates that there is considerable disorder [16].

5. Microtomed sections

Dlugosz and Keller [2] described the beam-induced changes in an ultramicrotomed section of spherulitic bulk PE as follows:

(i) An initially featureless specimen develops strong contrast corresponding to the spherulite banding observed in the optical microscope.

(ii) The contrast developed is lower in off-diametral sections.

(iii) It is the transparency of the lighter regions which is reduced when the sections are off-diametral, and the opacity of the darker regions does not increase.

(iv) Spherulites become domed, and this is more noticeable when the band contrast is strong.

(v) The total transmissivity of an area increases by 15%.

(vi) The ultimate contrast is greater for high initial dose rates.

(vii) In the scanning electron microscope, the specimen surface becomes undulating, but remains flat.

The differences between these observations and those described in this paper can be ascribed to the greater thickness of the specimens, or the presence of off-diametral sections. The authors suggested that the initial diffraction contrast was swamped by the continuous scatter from the section (observation i), since a diffracting unit will extend over only a small fraction of the specimen thickness. In off-diametral sections, as the radial growth direction rises further out of the specimen plane, the lamellae become increasingly "end-on" and the periodic variation in lamellar orientation along the radius of the section will be more and more limited. This in itself accounts for the lowered band contrast (observation ii). The model presented in this paper agrees with this, as "end-on" lamellae will behave in the same way as "edge-on" lamellae, whatever their orientation about the b-axis. In addition it can now be seen that observation (iii), that the highest transparency of lighter bands is reached in the diametral sections, is sufficient to show that the section thins most where the lamellae are in the "flat-on" position.

As mentioned in Section 4.2, an area of exactly "end-on" lamellae will contract in the specimen plane, and remain flat, so that a two-dimensional spherulite should have a flattened top to its conical shape after irradiation. This flattening effect extends over the whole area of an off-diametral section, and the predicted result is a dome. This dome will be more pronounced when the section is near the diametral plane, in agreement with the observations (ii) and (iv) above.

No dose rate dependent effect was found in the thin cast films, and their total transmissivity increased by less than 10%. A thick section, and the higher beam current which must be used can together give a significant temperature rise in the specimen, which might reduce constraints and so increase the final contrast (observation vi). The transmissivity, T, of a film of thickness t is given by $\exp(-t/\tau)$ where τ is a constant. This non-linear dependence on t means that if material in a uniform film is rearranged to give some thin areas and some thick areas, T will increase although the total mass is constant. The increase in T will be greater for thicker films.

If the electron beam in the scanning electron microscope does not completely penetrate the thin films, as in Fig. 10, then there will be a layer of undamaged polyethylene on the lower surface of the sections. This will act as a stabilizing restraint on the rest of the specimen so that large scale deformations are prevented. Local deformations, smaller than the penetration depth of the electrons, will not be affected (observation vii).

6. Conclusions

The model behaviour of crystalline lamellae described in Part 1 [1], applied to the accepted model of spherulite structure, has explained all the observations made. The dimensional changes of spherulitic films in the electron microscopes are in quantitative agreement with the predictions of the model. The contrast changes of both thin cast films and ultramicrotomed sections are qualitatively predicted by it. This is strong support for the twisting lamellar texture of spherulites, and inspires confidence that the same model behaviour of crystalline lamellae can be applied to interpret electron micrographs of unknown textures in polyethylene.

Acknowledgement

One of us (D. T. Grubb) wishes to acknowledge the support given by the "Procurement Executive", Ministry of Defence, for this work.

References

1. D. T. GRUBB, A. KELLER, and G. W. GROVES, *J. Mater. Sci.* **7** (1972) 131.
2. J. DLUGOSZ and A. KELLER, *J. Appl. Phys.* **39** (1968) 5776.
3. A. KELLER, *J. Polymer Sci.* **17** (1955) 291.
4. F. P. PRICE, *ibid* **37** (1959) 71.
5. H. D. KEITH and F. J. PADDEN, *ibid* **39** (1959) 101.
6. A. KELLER, *ibid* **39** (1959) 151.
7. A. KELLER and D. C. BASSETT, *Proc. Roy. Microscopic Soc.* **79** (1960) 243.
8. G. C. CLAVER, R. BUCHDAHL, and R. L. MILLER, *J. Polymer Sci.* **20** (1956) 202.
9. P. H. GEIL, "Polymer Single Crystals", (Interscience, New York, 1963) p. 229.
10. E. H. ANDREWS, M. W. BENNETT, and A. MARKHAM, *J. Polymer Sci.* A-2, **5** (1967) 1235.
11. H. D. KEITH and F. J. PADDEN *ibid* **39** (1959) 123.
12. D. T. GRUBB, *J. Phys. E.: Sci. Instrum*, **4** (1971) 222.
13. A. W. AGAR, F. C. FRANK, and A. KELLER, *Phil. Mag.* **4** (1959) 32.
14. J. W. HEAVENS, A. KELLER, J. M. POPE, and R. M. ROWELL *J. Mater. Sci.* **5** (1970) 53.
15. A. KELLER and S. SAWADA, *Makromolek. Chem.* **74** (1964) 190.
16. J. DLUGOSZ, private communication.

Received 25 November 1971 and accepted 7 January 1972.